ENERGETIKA. 2010. T. 56. Nr. 3–4. P. 254–259

Characterization of sol–gel auto-combustion derived spinel ferrite nano-materials

Andris Sutka,

Gundars Mezinskis,

Arturs Pludons,

Santa Lagzdina

Institute of Silicate Materials,
Azenes 14/24, LV-1048 Riga, Latvia
E-mail: gundarsm@ktf.rtu.lv

$CoFe_2O_4$, $NiFe_2O_4$ and ferrites $ZnFe_2O_4$ were prepared by the auto-combustion method. Scanning electron microscopy (SEM) was used for investigating the microstructural features of combustion reaction products. The structural evolution at different process stages of spinel ferrites are investigated by powder X-ray diffraction (XRD) and Fourier transform infrared techniques (FTIR). The XRD patterns of obtained products after calcination confirm the single-phase cubic spinel type. The average crystallite sizes for different compounds were found to be in nanometer range. The FTIR studies show two fundamental absorption bands which are assigned to the vibration of tetrahedral and octahedral complexes of the spinel structure. The powder-specific surface area was measured using the multi-point Brunauer–Emmet–Teller method (BET). The BET results show that after calcination submicrometer-sized primary particles have been agglomered into larger secondary particles. Atomic force microscopy (AFM) was used to study the dimensions of calcined ferrite particles. AFM images show that particles are of nanometer dimensions. Room temperature D. C. electrical conductivity measurements of the spinel ferrites show that the obtained compounds are of lower coductivity compared with spinel ferrites obtained by the conventional ceramic technique.

Key words: spinel ferrite, nanoparticles, combustion reaction, atomic force microscopy

1. INTRODUCTION

Nano-sized spinel ferrite nanoparticles are perspective materials for modern industries and technologies such as electrical engineering, electronics and information. Ferrites made from nanoparticles can show different properties unlike those observed in bulk material. The different properties of these materials can be attributed to the small size, a large surface-to-volume ratio, cation distribution, concentration of localized electric charge carriers, and stoichiometry. For these reasons, unusual electric and magnetic properties of nano-sized spinel ferrites can be observed [1].

The spinel ferrite structure with the general formula AB_2O_4 can be described as a cubic close-packed arrangement of oxygen atoms, which contains eight A-sites where metal cations are coordinated tetrahedrally, and sixteen B-sites which posses an octahedral coordination. When sublattice A contains Me^{2+} ions and sublattice B contains Fe^{3+} ions, the ferrite has a normal spinel structure. If the A-sites are completely occupied by Fe^{3+} ions and B-sites are randomly taken up with Me^{2+} and Fe^{3+}, the structure is attributed to an inverse spinel. In mixed spinel ferrites, both divalent and trivalent cations are distributed between A and B sites [2].

The bulk zinc ferrite posses a normal spinel structure where the A site contains all the Zn^{2+} ions. In $NiFe_2O_4$, the nickel ion, due to its superior radius (0.74 Å) [3] in comparison with Fe^{3+} radius (0.67 Å) [1], tends to occupy B sublattice states by making an inverse spinel structure [4]. Recent investigations have shown that cation distribution in nanosized $ZnFe_2O_4$ and $NiFe_2O_4$ is partly inverted, which means that both sites contain Me^{2+} and Fe^{3+} cations [5, 6]. $CoFe_2O_4$ forms an inverse spinel structure and, independently of the preparation technique and particle size, it has a high magnetic anisotropy and saturation magnetization [7].

The mentioned structural modifications of nanosized spinel ferrite materials increase its potential technological applications, thus an effective, simple method with a low energy consumption is significant. The preparation method strongly affects not only the size of ferrite powders, but also their properties; thus, the aim of the present paper was to demonstrate the properties of various spinel ferrites obtained by the sol–gel auto-combustion method.

2. METHODOLOGY

In order to obtain zinc, nickel and cobalt ferrites, metal nitrates as iron nitrate ($Fe(NO_3)_3 \cdot 9H_2O$), nickel nitrate ($Ni(NO_3)_2 \cdot 6H_2O$), zinc nitrate ($Zn(NO_3)_2 \cdot 6H_2O$) or cobalt nitrate ($Co(NO_3)_2 \cdot 6H_2O$) were dissolved in distilled water. Also, one mole of citric acid monohydrate ($C_6H_8O_7 \cdot H_2O$) was added to nitrate solution. Ammonia water (NH_4OH) was added to the prepared solution to addjust the pH value to 7. Then a highly viscous gel was formed after intensive stirring and evaporation at 100 °C. The resulting gel was heated up to 250 °C to initiate combustion; as a result, as-burnt product powder mixture of different oxide compounds was obtained. The obtained oxide mixture was calcinated at 800 °C for 1 h.

The XRD patterns of the combustion reaction and annealed powders were recorded for 2θ from 5° to 60° at a scan rate of 2° min^{-1} using an X-ray Rigaku Ultima+ diffractometer with $Cu_{K\alpha}$ radiation (λ = 1.5418 Å).

The IR absorption spectra of calcinated powders were recorded in the wave number range of 4000–400 cm^{-1} with a Shimadzu Prestige-21 spectrometer. Sample preparation for FTIR measurements included mixing ferrite powder with potassium bromide (KBr) powder.

Microstructural features of as-burnt powders were characterized with a SEM Hitachi TM 1000. The particle dimensions of calcinated ferrite powders were collected with a Digital Instruments CP-II scanning probe microscope, Veeco Instruments Inc., by the non-contact mode. The particle size was determined by AFM topographical analysis, taking into account at least 100 particle diameters. Samples for AFM analysis were prepared by dispersing ferrite particles in heptane with a subsequent ultrasound treatment to destroy particle aglomerates and agregates. A drop of dispersion onto a mica sheet was analyzed after drying.

The specific surface area was determined by the physical adsorption of N_2 employing the multi-point BET calculation method and using a Surface Area and Pore Size Analyser NOVA 1200e.

DC resistivity measurements were performed by the two-probe method with a E6-13A tera-ohmmeter. Samples for resistivity measurements were made in the form of tablets 1 mm thick and 10 mm in diameter. Tablets were pressed from auto-combustion reaction products at a pressure of 20 MPa, using 5 wt% propanol-2 as a binder. The pellets were sintered / calcinated at 1100 °C for 2 hours. To ensure good electric contacts, the samples were painted on either side with a high purity conductive silver paint.

3. RESULTS AND DISCUSSION

3.1. X-ray studies

The X-ray diffraction patterns of as-burnt and calcined $CoFe_2O_4$, $ZnFe_2O_4$, and $NiFe_2O_4$ ferrite samples are presented in Fig. 1.

The XRD patterns of as-burnt products, besides the cubic spinel structure, indicate the presence of other minor phases caused by impurities. At 800 °C calcined products contain single-phase $ZnFe_2O_4$, $NiFe_2O_4$ and $CoFe_2O_4$ spinel. The

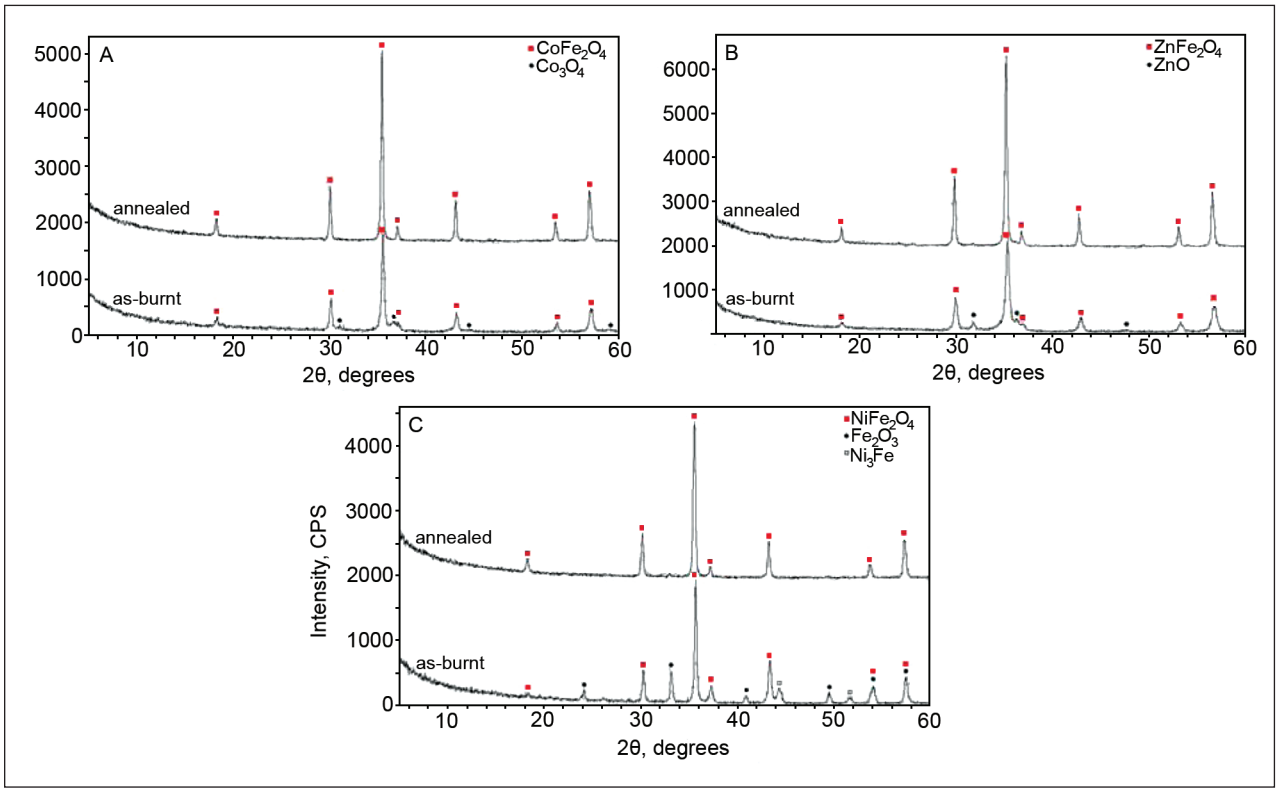

Fig. 1. XRD pattern of as-burnt and calcined powders: A – $CoFe_2O_4$; B – $ZnFe_2O_4$; C – $NiFe_2O_4$

Table. **Various properties of obtained ferrite powders**

Ferrite	D, nm	V_1, cm^{-1}	V_2, cm^{-1}	Specific surface area, m^2/g	σ, Ω^{-1} · cm^{-1}
As-burnt $ZnFe_2O_4$	20	548	409	36	–
Calcined $ZnFe_2O_4$	35	550	413	8	1.83E-06
As-burnt $NiFe_2O_4$	28	579	–	36	–
Calcined $NiFe_2O_4$	33	584	–	5	1.22E-06
As-burnt $CoFe_2O_4$	24	578	–	33	–
Calcined $CoFe_2O_4$	35	586	–	25	2.26E-07

crystallite size (Table), determined by using Debye–Scherrer equation, for differently prepared ferrite compounds is at nanometer dimensions and increases with taking calcination at 800 °C. The lattice parameter *a* of the as-burnt and calcined ferrites was determined by using the following formula [9]:

$$a = \frac{\lambda}{2}\frac{\left(h^2 + k^2 + l^2\right)^{1/2}}{\sin\theta}, \quad (1)$$

where λ is the wavelength of Cu*K*α, (hkl) are the Miller indices, and θ is the diffraction angle of a corresponding (hkl) plane. Parameter *a* was calculated from the (220) plane due to its amenability by changes in both A and B sites as concluded by He et al. [10].

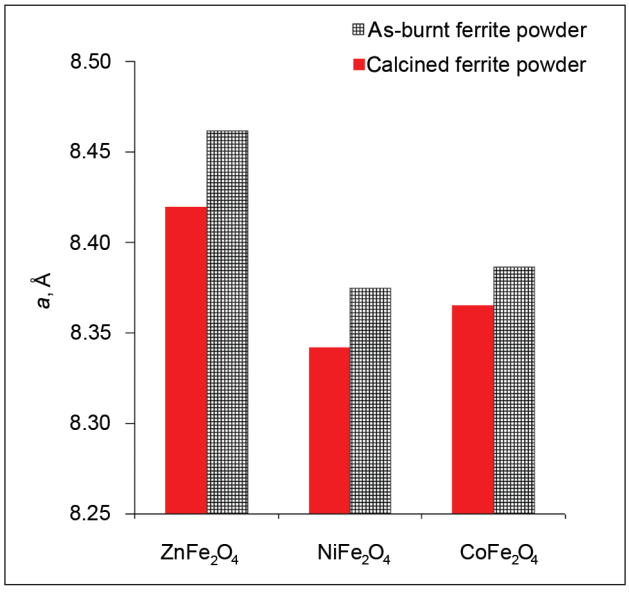

Fig. 2. Changes in lattice parameter by calcination at 800 °C of obtained spinel ferrites

The lattice parameter in all cases increases by ferrite treatment at an elevated temperature (Fig. 2); this suggests the formation of a compositionally stoichiometric spinel ferrite [9]. The observed lattice parameter values for calcined ferrites are in good agreement with the results for nanosized ferrites obtained by other authors [11, 12].

3.2. Fourier transmission infrared spectroscopy studies

From FTIR results presented in Table we can observe typical spinel ferrite absorption bands which are attributed to metal–oxygen vibrations. The first one, V_1, mostly noticed in the range between 600–540 cm^{-1} [13], corresponds to intrinsic stretching vibrations at the tetrahedral site, and the second one, V_2, is observed in the diapason 450–385 cm^{-1} which corresponds to the octahedral site [11]. These absorption bands are highly sensitive to changes in interaction between oxygen and cations, as well as to the size of the obtained nano-particles [13].

The observed V_1 bands (Table) in all cases were higher for calcined samples due to formation of stoichiometric ferrite, as well as Fe^{3+} ion replacement with Zn^{2+}, Ni^{2+} or Co^{2+}.

For $NiFe_2O_4$ and $CoFe_2O_4$ ferrites, we could not observe an accurate value of V_2 vibrations because the spectra were recorded in the range of 4000–400 cm^{-1}, but octahedral site vibrations for these samples were located below 400 cm^{-1}.

3.3. Microscopy studies

From the SEM image (Fig. 3) one can see that durig the autocombustion reaction highly porous and fluffy products are formed. Also, sub-micrometer-sized primary particles are agglomerated into larger secondary particles. The shape and size of individual particles cannot be determined from the obtained micro-photograph.

Non-contact AFM topographical images and topographical analysis of $ZnFe_2O_4$, $NiFe_2O_4$ and $CoFe_2O_4$ are shown in Fig. 4. As we can see, ferrite powders consist of individual particles and superior sized clusters which consist of smaller individual particles as was concluded by Dias et al. [14].

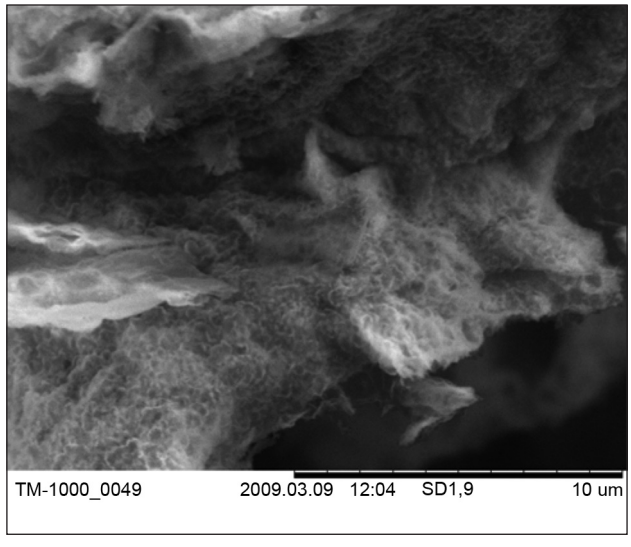

Fig. 3. SEM microphotography of the $CoFe_2O_4$ as-burnt powder

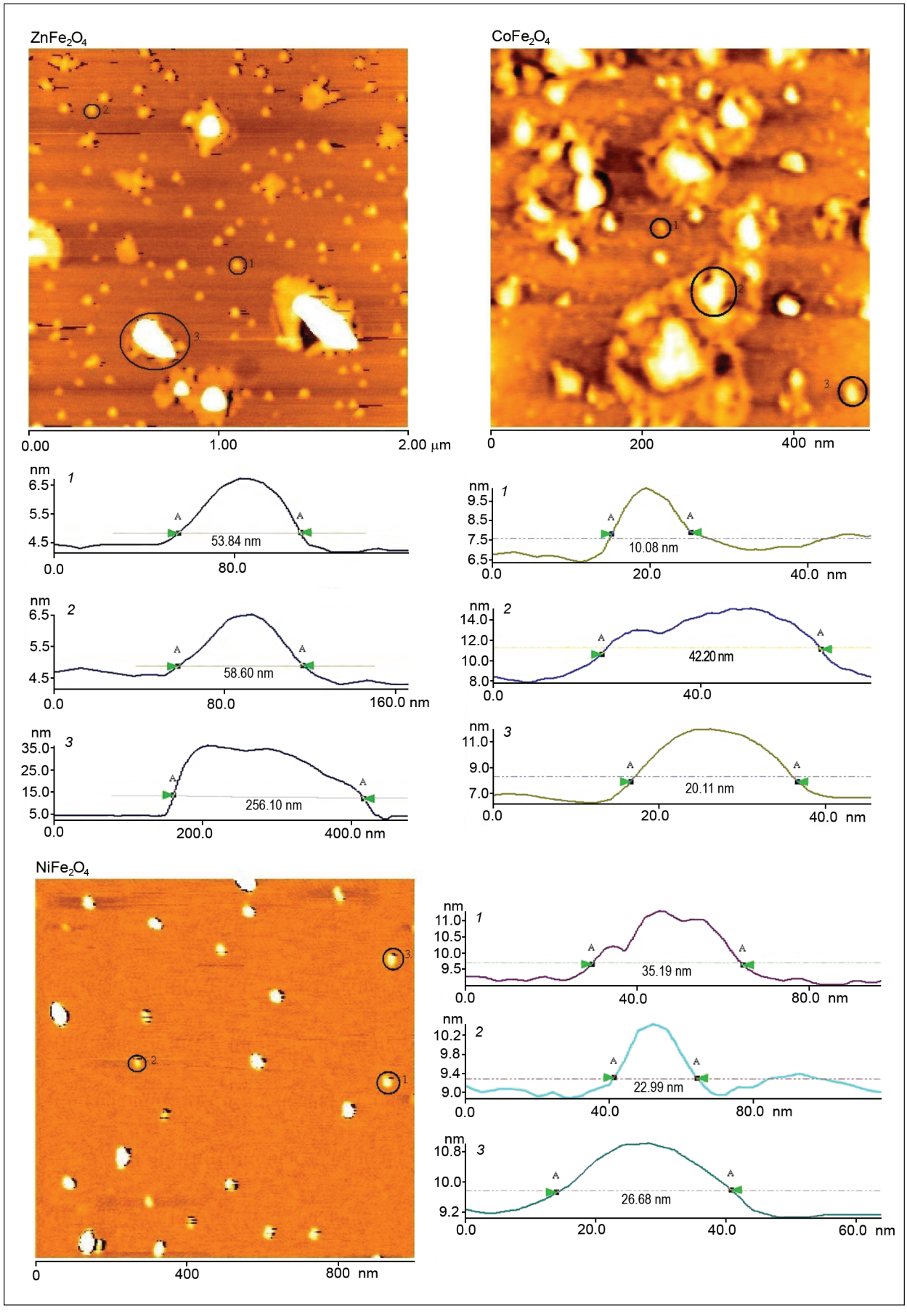

Fig. 4. AFM topographical image and topographical analysis of ferrite powders

Particle sizes for $ZnFe_2O_4$ were 25–70 nm, for $NiFe_2O_4$ 10–45 nm and for $CoFe_2O_4$ 10–40 nm. In the case of $ZnFe_2O_4$, there were larger particles and particle clusters. Higher zinc ferrite average particle and cluster sizes are due to the Zn^{2+} ion which to increase the combustion reaction temperature, resulting in an intensified individual particle growth [15], as well as liquid phase presence of zinc in the sintering process, attributed to its low melting point (470 °C), which draws the particles together because of capillary forces [16].

From the specific surface area of as-burnt powders (Table) we can see that as-burnt powders have a mesoporous character. As a result of calcination, the products showed a clear decrease of the surface areas because sub-micrometer-sized primary particles have been agglomerated into larger secondary particles.

3.4. Conductivity

The measured electrical conductivity values are shown in Table. The comparetively low conductivity values, due to spinel ferrites, belong to the group of so-called hopping semiconductors in which the basic conduction mechanism is attributed to the hopping of electrons from one cation to another [17] and not due to the thermal creation of charge carriers.

In general, the observed electrical conductivity was lower than that for ferrites obtained by the convectional ceramic technique, attributed to small-grain sizes and a larger number of insulating grain boundaries which act as barriers to the flow of electrons [18].

4. CONCLUSIONS

To sythesize nanosized Ni–Zn ferrite powders, the combustion sythesis method was used. The FTIR studies and lattice parameter changes show that by annealing at 800 ºC, compositionaly stoichiometric ferrite compounds are formed. The topographical images obtained by AFM indicate that ferrite powders consist of nanometer-sized individual particles and of particle clusters.

ACKNOWLEDGMENTS

The scientific investigations and results presented in this paper were financed by the European Social Fund.

Received 15 July 2010
Accepted 11 October 2010

References

1. Gul I. H., Ahmed W., Maqsood A. Electrical and magnetic characterization of nanocrystalline Ni–Zn ferrite synthesis by co-precipitation route. *Journal of Magnetism and Magnetic Materials*. 2008. Vol. 320. P. 270–275.
2. Daliya S. M., Ruey-Shin J. An overview of the structure and magnetism of spinel ferrite nanoparticles and their synthesis in microemulsions. *Chemical Engineering Journal*. 2007. Vol. 129. P. 51–65.
3. El-Sayed A. M. Influence of zinc content on some properties of Ni–Zn ferrites. *Ceramics International*. 2002. Vol. 28. P. 363–367.
4. Paiva J. A. C., Graca M. P. F., Macedo M. A., Valente M. A. Spectroscopy studies of $NiFe_2O_4$ nanosized powders obtained using coconut water. *Journal of Alloys and Compounds*. 2009. Vol. 485. P. 637–641.
5. Wang Z., Schiferl D., Zhao Y., O'Neill C. High pressure Raman spectroscopy of spinel-type ferrite $ZnFe_2O_4$. *Journal of Physics and Chemistry of Solids*. 2003. Vol. 64. P. 2517–2523.
6. Chinnasamy C. N., Narayanasamy A., Ponpandian N., Joseyphus J. R., Jeyadevan B., Tohji K., Chattopadhyay K. Grain size effect on the Neel temperature and magnetic properties of nanocrystalline $NiFe_2O_4$ spinel. *Journal of Magnetism and Magnetic Materials*. 2002. Vol. 238. P. 281–287.
7. Chinnasamt C. N., Senoue M., Jeyadevan B., Perales-Perez O., Shinoda K., Tohji K. Synthesis of size-controlled cobalt ferrite particles with high coercivity and squareness ratio. *Journal of Colloid and Interface Science*. 2003. Vol. 263. P. 80–83.
8. Costa A. C., Tortella E., Morelli M. R., Kaufman M., Kiminami R. H. Effect of heating conditions during combustion synthesis on the characteristics of $Ni_{0.5}Zn_{0.5}Fe_2O_4$ nanopowders. *Journal of Materials Science*. 2002. Vol. 37. P. 3569–3572.
9. Hwang C. C., Tsai J. S., Huang T. H., Peng C. H., Chen S. Y. Combustion synthesis of Ni–Zn ferrite powder-influence of oxygen balance. *Journal of Solid State Chemistry*. 2005. Vol. 170. P. 382–389.
10. He X., Song G., Zhu J. Non-stoichiometric NiZn ferrite by sol-gel processing. *Materials Letters*. 2005. Vol. 59. P. 1941–1944.
11. Mouallem-Bahout M., Bertrand S., Pena O. Synthesis and characterization of $Zn1\text{-}xNixFe_2O_4$ spinels prepared by a citrate precursor. *Journal of Solid State Chemistry*. 2005. Vol. 178. P. 1080–1086.
12. Sileo E. E., Rodenas L. G., Paiva-Santos C. O., Stephens P. W., Morando P. J., Blesa M. A. Correlation of reactivity with structural factors in a series of Fe(II) substituted cobalt ferrites. *Journal of Solid State Chemistry*. 2006. Vol. 179. P. 2237–2244.
13. Marykutty T., George K. C. Infrared and magnetic study of nanophase zinc ferrite. *Indian Journal of Pure & Applied Physics*. 2009. Vol. 47(1). P. 81–86.
14. Dias A., Buono V., Vilela J., Andrade M., Lima T. Particle size and morphology of hydrothermally processed MnZn ferrites observed by atomic force microscopy. *Journal of Materials Science*. 1997. Vol. 32. P. 4715–4718.
15. Costa A., Silva J., Cornejo D., Morelli M. Magnetic and structural properties of $NiFe_2O_4$ ferrite nanopowder doped with Zn^{2+}. *Journal of Magnetism and Magnetic Materials*. 2008. Vol. 320. P. e370–e372.

16. Ajmal M., Maqsood A. AC conductivity, density related and magnetic properties of $Ni_{1-x}Zn_xFe_2O_4$ ferrites with the variation of zinc concentration. *Materials Letters*. 2008. Vol. 62. P. 2077–2080.
17. Mangalaraja R., Manohar A., Gnanam F. Direct current resistivity studies of $Ni_{1-x}Zn_xFe_2O_4$ prepared through flash combustion and citrate gel decomposition techniques. *Materials Letters*. 2003. Vol. 57. P. 2662–2665.
18. Rao B. P., Rao K. H. Effect of sintering conditions on resistivity and dielectric properties of Ni–Zn ferrites. *Journal of Material Science*. 1997. Vol. 32. P. 6049–6054.

Andris Sutka, Gundars Mezinskis, Arturs Pludons, Santa Lagzdina

FERITINIŲ ŠPINELIŲ, GAUTŲ SAVAIMINIO DEGIMO METODU, CHARAKTERISTIKOS

S a n t r a u k a

$CoFe_2O_4$, $NiFe_2O_4$ ir feritas $ZnFe_2O_4$ buvo gauti savaiminio degimo metodu. Degimo reakcijos produktų mikrostruktūrinėms savybėms tirti buvo panaudota skenuojanti elektroninė mikroskopija (SEM – *Scanning elektron microscopy*). Skirtingais proceso etapais struktūrinė špinelių feritų raida buvo tiriama rentgeno spindulių difrakcija (XRD – *X-ray diffraction*) ir Furjė transformacine infraraudonųjų spindulių technika (FT-IR – *Fourier transform infrared techniques*). Gautų produktų XRD vaizdas po kalcinacijos atitinka vienfazį kubinio špinelio tipą. Skirtingų junginių kristalitai ne didesni nei nanometras. FT-IR tyrimai parodė dvi pagrindines sugėrimo juostas, priskiriamas ketursienių ir aštuonsienių špinelio struktūros kompleksų vibracijai. Specialiais milteliais padengto paviršiaus sritis buvo matuojama daugiataškiu Brunauer–Emmet–Teller metodu (BET). BET tyrimo rezultatai parodė, kad po kalcinacijos pirminės mikrometrinės dalelės buvo sukauptos į didesnes antrines daleles. Kalcinuotų feritų dalelių matmenys buvo tiriami atominės jėgos mikroskopija (AFM – *Atomic force microscopy*). AFM vaizdai rodo, kad dalelės yra nanometro ribose. Špinelių struktūros feritų DC elektros laidumo matavimai parodė, kad gautieji junginiai mažina laidumą, palyginti su feritais, gautais įprastiniu keraminiu būdu.

Raktažodžiai: feritiniai špineliai, nanodalelės, degimo reakcija, atominės jėgos mikroskopija

Андрис Сутка, Гундарс Мезинскис, Артурс Плудонс, Санта Лаздиня

ХАРАКТЕРИСТИКИ ФЕРРИТОВЫХ ШПИНЕЛЕЙ, ПОЛУЧЕННЫХ МЕТОДОМ СОБСТВЕННОГО ГОРЕНИЯ

Р е з ю м е

$CoFe_2O_4$, $NiFe_2O_4$ и феррит $ZnFe_2O_4$ были получены методом собственного горения. Для исследования свойств микроструктурных продуктов горения использована сканирующая электронная микроскопия (SEM – *Scanning elektron microscopy*). На различных этапах процесса структурное развитие шпинелей ферритов исследовалось с помощью рентгеновской дифракции (XRD – *X-ray diffraction*) и Фурье трансформационной техникой инфракрасных лучей (FT-IR – *Fourier transform infrared techniques*). Вид полученных продуктов (XRD) после процесса кальцинации соответствует типу однофазного кубического шпинеля. Величина кристаллитов различных соединений не превышает одного нанометра. Исследования FT-IR показали две основные полосы (зоны) поглощения, соответствующие вибрации четырех- и восьмигранных структурных комплексов шпинелей. Область поверхности, покрытая специальными порошками, исследовалась многоточным методом Брунауер–Еммет–Теллер (BET). Результаты этого исследования показали, что после кальцинации первичные частицы (величина – микрометр) были сконцентрированы в больших вторичных частицах. Размеры кальционированных частиц ферритов исследовались микроскопией атомных сил (AFM – *Atomic force microscopy*), где получено, что частицы по величине остаются в пределах нанометра. Измерения электропроводности шпинелей (DC) показали, что полученные соединения уменьшают электропроводность по сравнению с ферритами, полученными обыкновенным керамическим методом.

Ключевые слова: ферритовые шпинели, наночастицы, реакции горения, микроскопия атомных сил